Low coherence full field interference microscopy or optical coherence tomography: recent advances, limitations and future trends

I. Abdulhalim

I. Abdulhalim, "Low coherence full field interference microscopy or optical coherence
tomography: recent advances, limitations and future trends," Proc. SPIE 8788, Optical Measurement Systems for Industrial Inspection VIII, 878802 (13 May 2013); doi: 10.1117/12.2025199

SPIE.

Event: SPIE Optical Metrology 2013, 2013, Munich, Germany

Low coherence full field interference microscopy or optical coherence tomography: recent advances, limitations and future trends.

I. Abdulhalim
Department of Electrooptic Engineering and the Ilse Katz Center for Nano Scale Science and Technology, Beer Sheva 84105, Israel
abdulhlm@bgu.ac.il

ABSTRACT

Although low coherence microscopy (LCM) has been known for long time in the context of interference microscopy, coherence radar and white light interferometry, the whole subject has attracted a wide interest in the last two decades particularly accelerated by the entrance of OCT, as a noninvasive powerful technique for biomedical imaging. Today LCM can be classified into two types, both acts as three-dimensional imaging tool. The first is low temporal coherence microscopy; also known as optical coherence tomography (OCT), which is being used for medical diagnostics. The second is full field OCT in various modes and applied to various applications. FF-OCT uses low spatial and temporal coherence similar to the well-known coherence probe microscope (CPM) that have been in use for long time in optical metrology. The CPM has many advantages over conventional microscopy in its ability to discriminate between different transparent layers in a scattering medium thus allowing for precise noninvasive optical probing of dense tissue and other turbid media. In this paper the status of this technology in optical metrology applications will be discussed, on which we have been working to improve its performance, as well as its limitations and future prospective.

Keywords: Interference microscopy, full field optical coherence tomography, low coherence microscopy, Linnik microscope, Mirau Microscope

1. INTRODUCTION

The field of optical metrology has been[1] the drive for innovative optical measurement and diagnostic techniques over the years. The continuous requirement for more and more accurate measurements of thickness, step height and surface profiles led to the development of ellipsometry, polarized reflectometry and interferometry to allow sub-nm accuracy. Modulated spectroscopic and variable angle ellipsometry[2] techniques are capable of measuring sub-Angstrom variations in thickness and allow measuring refractive indices dispersion to accuracy better than 0.0001. With the advent of detector arrays the ease of building a setup and acquiring data in high speed enhanced the performance of optical metrology techniques (such as the CCD, CMOS camera, the parallel spectrometers). Image processing is playing a key role in enhancing optical microscopy as a quantitative measurement tool, due to the enhanced power of microprocessors. In the silicon microelectronic industry the optical microscope combined with a CCD camera, image processing and automatic scanning with nano scale accuracy is acting as a must for any fabrication facility. Among the most prominent applications are the inspection of overlay misregistration between two layers and the width of a line called critical dimension (CD) which represents the width of the transistor gate. Different optical microscopy modes have been in use for variety of layered structures[3,4,5]. Interference microscopy[6,7] was used when the layers are transparent to enhance the contrast of the image. Differential interference contrast (DIC) microscopy or Nomarski microscopy is being used for step height and surface profiling. Three dimensional images for lines were also obtained using the Linnik microscope system[8,9,10,11] from which CD and overlay were measured with nm accuracy. Dark field and polarized imaging are used when the edges are scattering, in order to enhance the edge detection. When the era of nano-electronics started, that is with the shrinkage of the design rules to the nano scale[12] (<200nm) the resolution limit for an optical microscope affected the measurement accuracy of the CD and overlay. This fact has led to the invention of optical spectroscopic scatterometry[13] as a powerful tool to measure line widths down to 20nm using visible and UV light[14] as well as for overlay measurement[15]. In its simplest configuration[16,17,18], optical spectroscopic scatterometry technique measures the reflectivity from zero order gratings versus wavelength and uses inverse scattering methodology to extract the lines width with sub-nm accuracy.

Optical Measurement Systems for Industrial Inspection VIII, edited by
Peter H. Lehmann, Wolfgang Osten, Armando Albertazzi, Proc. of SPIE Vol. 8788,
878802 · © 2013 SPIE · CCC code: 0277-786X/13/$18 · doi: 10.1117/12.2025199

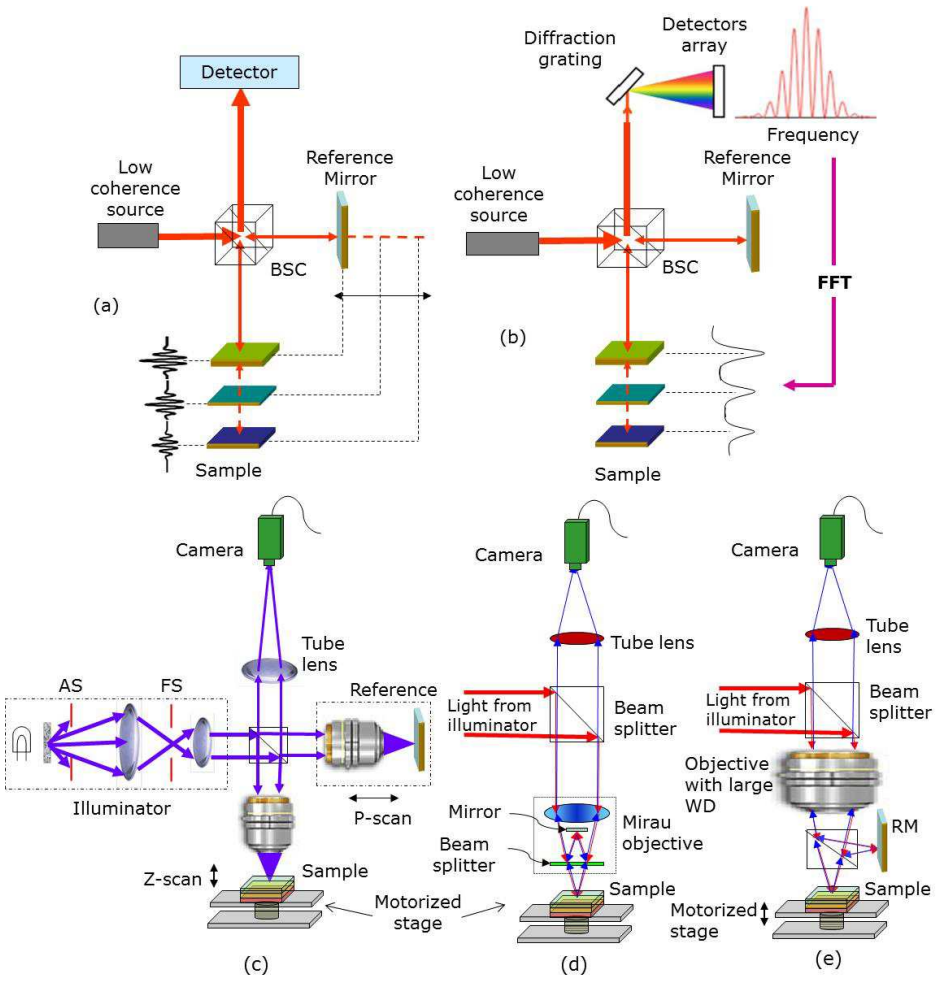

Figure 1. Schematic drawings of (a) time domain OCT setup, (b) frequency domain OCT setup, (c) Linnik microscope, (d) Mirau microscope and (e) Taylo microscope.

Interferometers based on lasers are being used for variety of optical metrology applications such as surface profiling, optical encoders for position measurement down to the Angstrom scale, characterization of optical surfaces in the lenses and mirrors production industry, and even gravitational waves detection. Another mode of interferometry consists of using broadband light source, historically called white light interferometry[19] (WLI) or coherence radar[20]. In WLI the short coherence length allows detecting interfaces within accuracy of half the temporal coherence length or even less when phase shift algorithms are used[21,22]. The principle of operation of WLI can be understood from figure 1a which describes a Michelson interferometer. Assuming the reference and sample beams are perfectly aligned one to the other, interference fringes are obtained on the detector as the reference or sample arm is scanned (P-scan stands for pathlength scanning) and the pathlength difference is less than the temporal coherence length. By scanning the sample in the transverse plane (XY) a 3D image of the sample is built. In its frequency domain mode the spectral interferogram is grabbed and analyzed with a spectrometer (figure 1b) and then Fourier transformed to reveal the layers interfaces of the structure. Fiber form[23] of the Michelson interferometer can be used for compactness and higher lateral resolution as the spot size from a single mode optical fiber can be brought down to the diffraction limit. To further increase the lateral resolution and obtain 3D images in one scan, microscope objectives can be incorporated both in the reference and sample arms to form what is known as the Linnik microscope[24] shown in figure 1c. When both the reference and sample objectives are in focus, interference occurs between the reference and sample images within an axial distance equals the coherence length. Variations on the Linnik microscope exist such as the Mirau microscope[25] and the Taylor microscope which offer nearly common path operation as shown in figures 1d and 1e respectively.

Optical coherence tomography (OCT) was introduced successfully in the early 1990's[26,27] as a powerful technique for applications in imaging of biological tissue. Since then the whole subject has gained a huge momentum both in tissue imaging and in other applications[28,29]. For some applications such as ophthalmology, cardiology and dermatology, OCT is being used in the clinics[30]. In principle OCT is nothing more than WLI except for the fact that high signal to noise ratio is required in order to observe the small signals of light scattered backward from tissue interfaces. This was achieved with the use of super-quiet light sources such as light emitting diodes (LEDs) and laser diodes (LD's) as well as the use of modulation and heterodyning techniques. Variety of OCT modes were introduced such as the time domain OCT (TDOCT) shown in figure 1a, frequency domain OCT (FDOCT) shown in figure 1b, polarization sensitive OCT (PSOCT), Doppler OCT (DOCT) and full field OCT (FFOCT). FDOCT relies[31,32,33,34] on acquiring the interference signal at each wavelength of the broadband source and Fourier transforming the spectral signal obtained, the resulting Fourier peaks represent the locations of the scattering interfaces along the depth of the sample. This mode of operation avoids the axial scan (Z-scan) thus improves the speed of 3D imaging. Using today miniature spectrometers and tunable lasers the FDOCT is becoming more popular. FFOCT is another mode for enhancing the 3D imaging speed by using lenses and microscope objectives to get interference between two 2D images rather than between two points. It is nothing more than the interference microscopy modes described in figures 1c-1e. It was used for imaging of biological tissue mainly using the Linnik microscope[35,36,37,38].

II. SOME RESULTS OF OPTICAL METROLOGY APPLICATIONS OF LCM

In our early experiments we have investigated the three types of interference microscopes: Linnik, Mirau and Taylor microscopes shown in figures 1c-1d. The light source used is a halogen lamp coupled to a fiber bundle. A diffuser is located near the fiber output to homogenize the beam and Kohler type illumination is used with possibilities to control field and aperture stops. In the Linnik microscope case the beam splitter cube generated the reference and sample beams which were focused on the reference mirror and the sample. Microscope objectives with different numerical apertures were used. The systems with high NA objectives (NA=0.9) were built at KLA-Tencor with the light source being a xenon arc lamp. In the Linnik microscope buildup, care should be taken to make sure the reference and sample paths contain similar amount of glass, which otherwise can produce dispersion errors[39] in particular when wideband source is used. For that matter the two objectives and beam splitter cube form a compensated set which needs to be selected before the system buildup starts. The Mirau microscope is a common path interference microscope in that the reference mirror is located inside the objective in a plane conjugate to the object plane. The Mirau objective used is Nikon x10 with numerical aperture NA=0.3. The sample is setting on a stage connected to a step motor for Z scanning that is controlled by computer with 20nm resolution. The camera located at the image plane and synchronized to start grabbing images during the Z scan in a predetermined time interval. The Taylor microscope is referred to also as the Michelson microscope in which the two Michelson interferometer arms are imaged using a single microscope objective. The disadvantage of this configuration is that only large working distance objectives can be used and the aberrations that can be introduced by the beam splitter in the focused beam. To minimize aberrations effects we used an achromatic triplet Hastings lens (Edmunds NT30-229) as an objective corrected for spherical, distortion and chromatic aberrations for the visible range of the spectrum and has large working distance.

As an interferometric microscope, FF-OCT had the primary function of contrast enhancement when samples of low contrast are to be imaged. Assuming a layered structure with low contrast is within the focal depth of the microscope objective, a bright field image can barely distinguish between the two layers. However an interferometric image transforms the thickness and refractive index variations into phase difference that improves the contrast in a similar manner to phase contrast microscopy. In figure 2 an example of overlay target image is shown using bright field and interference microscope with NA=0.9. Overlay misregistration is an optical metrology application important in the micro- and nano-electronics industry. During the lithography processes, the Si technology manufacturers produce square like marks in each layer and the function of the optical metrology tool is to measure the misalignment or misregistration between them. For the case of a square-in-square target (or so called box in box target), the inner and outer boxes correspond to the bottom and top layers respectively while the difference between their centers is simply the misregistration. Figure 2b shows a strong enhancement of the edge contrast as compared to the bright field image in figure 2a. Because the contrast depends on the phase difference between the sample and reference beam, the phase was varied by performing P-scan and the image in the enhanced region built synthetically. Assuming the objectives at the

same Z, then $\delta z = 0$ and so one can distinguish between two cases with high contrast variation $\varphi_0 = 0$ or $\varphi_0 = \pi$. Hence the best contrast is achieved when the beams reflected from the two layers are out of phase.

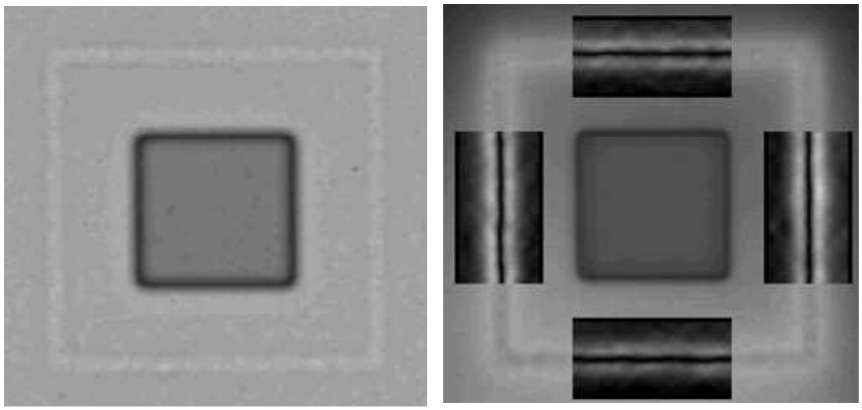

(a) Bright Field Microscope Image (b) Interference Microscope Image

Figure 2. Box in box overlay misregistration targets imaged with (a) bright field microscopy, (2) Linnik microscope.

Surface profiling, step height and critical dimension (CD) measurements are among the popular applications of TD-FFOCT in the nano-technology industry. Figure 3b shows a synthetic image showing a cross section of resist line on Si (figure 3a). Upon performing Z scan, an interferogram is obtained when the pathlength difference between the reflected beam from the sample and the reference beam is within the coherence region. Hence the 1st and 2nd interferograms shown in figure 3b correspond to the top and bottom interfaces of the resist line. The line height is then found by finding the difference between the center of mass of the two interferograms or by using correlation function. Figure 3c shows another example of cross section from a structure obtained as part of the process for CMOS manufacturing. Subwavelength features in the metal surface are also seen, demonstrating the high axial and lateral resolution when FF-OCT is used with high NA objectives. It should be noted here that when using high NA objectives one can rely on the low spatial coherence and use a long temporal coherence source such as a laser. This has the advantage of simplifying the algorithms for determining the layers thicknesses as refractive index dispersion is then avoided. One can rely on the fact that the fringe size is also well known for monochromatic light to precisely calibrate the system. The fringe size and its dependence on the spatial coherence was discussed by us in previous works[10,11]. Another possible simplification is to use annular lenses where one can then ignore the angular spectrum if the annulus width is small enough. The interferogram for the case of annular lens is given by[40]:

$$I(\delta z) = 0.5 + \frac{\sqrt{R_r R_s}}{R_r + R_s} sin\, c(kNA^2(1-\varepsilon^2)\delta z/4)\, sin\, c(k(cos\,\theta_\varepsilon - cos\,\theta_{max})\delta z)$$
$$cos(k(cos\,\theta_\varepsilon + cos\,\theta_{max} - NA^2(1+\varepsilon^2)/4)\delta z + \varphi_0) \quad (1)$$

Where the central obscuration ratio is denoted by ε and defined as the ratio of the radius of the obscuration disc to the radius of the full aperture. The light angular interval collected by each objective is between θ_ε and θ_{max} where $\theta_\varepsilon = \varepsilon NA$. Figure 4a shows that using NA=0.9 and narrow annulus, one can still get submicron axial resolution even using a monochromatic light. This is an interesting result as it demonstrates that the lateral spatial coherence length remains short enough when the NA is high even if the obstruction ratio is as high as $\varepsilon = 0.9$.

Another interesting application of FF-OCT is thin film thickness mapping. In a similar manner to step height measurement and surface profiling, thin films thickness can be measured using TD-FFOCT and FD-FFOCT. Using a camera one can then build a thickness map with high lateral and axial resolution. An attempt in this direction has already been implemented with WLI[41]. Figure 4b shows TD-FFOCT interferogram from a 2.5μm thick silicon oxide layer on Si substrate obtained from a an area of 40x40 pixels which with x10 magnification corresponds to an area of

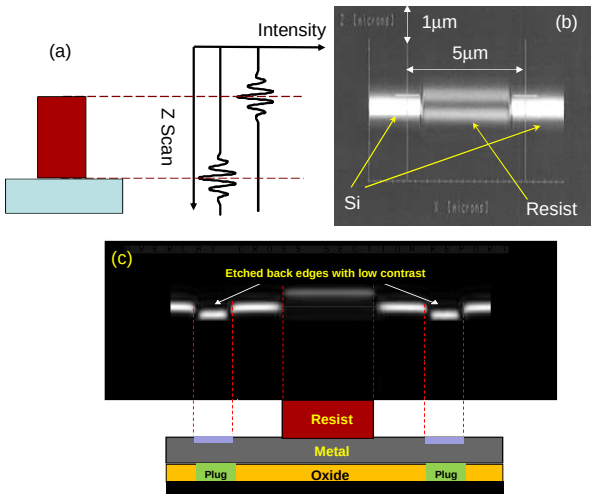

Figure 3. Demonstration of cross section images obtained with the Linnik microscope: (a) Resist line on Si drawing and (b) Its cross section, (c) show the cross section of a more complicated structure after etch back process.

approximately 15x15µm^2 on the sample. Using a fiber optic spectrometer the spectroscopic interferogram was grabbed as shown in figure 5a and Fourier transformed to reveal the layer thickness without any mechanical scanning as shown in figure 5b. The entrance fiber diameter of 400mm corresponds to 40µm diameter area on the sample was located in the image plane. The Mirau objective used here has NA=0.3 and so the spatial coherence length is approximately 9µm, much larger than the SiO_2 layer thickness. The short temporal coherence length (about 1µm) used here allowed us to measure such a thin layer. Figures 4 and 5 both reveal a layer thickness of ~2.5µm as expected. Note that although we have used a lens with NA=0.3, we obtained an excellent accuracy even with FD-OCT. This is believed to be the case for NA as large as 0.7 but above 0.7 some correction needs to be considered because of the angular dependence of the pathlength. The FD-OCT is expected to work best when there is one spatial frequency by a continuum of temporal frequencies. Here we have proved that it is possible to use FD-OCT even with a continuum of spatial frequencies. This fact allows building FF-OCT systems to obtain a high resolution thickness map without any mechanical scanning by combining a tunable filter or a tunable laser source in conjunction with a camera to grab spectral interferometric images.

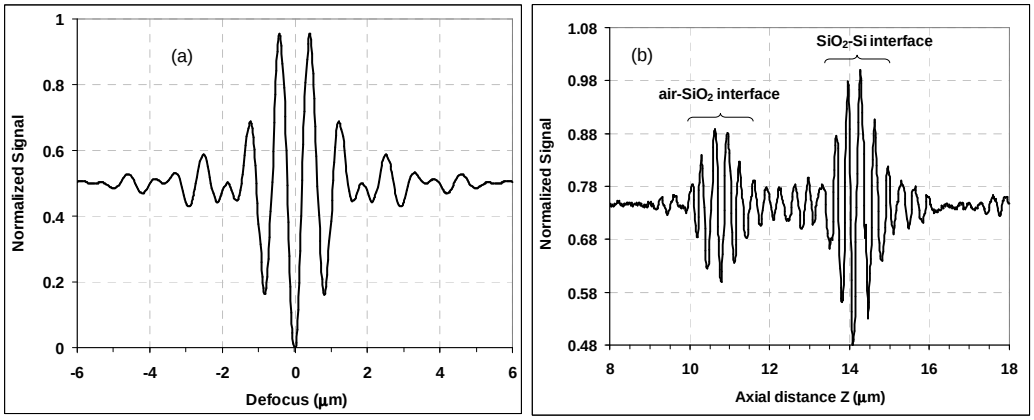

Figure 4. (a) Calculated interferrogram from a Linnik microscope with annular lenses having large obstruction ratio and (b) Interferograms obtained experimentally from SiO2 layer on Si using Mirau microscope.

A question of interest is what are the advantages of using OCT compared to ellipsometry and polarized reflectometry for thin films measurement?. Although ellipsometry contains information on the phase and the polarization which is why it gives high resolution down to sub-nm, usually it is bulky and requires phase modulator or mechanical rotation of polarizer. Reflectometry is less accurate because it is an intensity measurement and therefore it is limited by the noise of the source. OCT in this sense can have better accuracy than reflectivity because it is interferometric and therefore contains some phase information. The question then is how to design an OCT system for thin film measurements that

competes with the above two techniques. For very thin layers the axial resolution though cannot compete with spectroscopic ellipsometry or polarized reflectometry because the shortest possible coherence length is limited to a half wavelength. Nevertheless for micron or more thick layers this is possible using visible light in particular if the multiple interferences are negligible such as the case with scattering layers. For scattering layers the criterion for axial resolution being used in tissue imaging with OCT is to have the layers thicknesses larger than half the coherence length. The question is how this criterion changed when the layers are non-scattering and multiple interferences take place?. It is clear that when the films thickness is smaller than the coherence length and interface reflections are strong, multiple interferences have a strong effect on the interferogram. The determination of the center of mass of the interferograms is less accurate. When FD-FFOCT is used, additional Fourier peaks appear due to multiple reflections (figure 6a) which can ruin the measurement accuracy as shown in figure 6b when the coherence length longer than the layer thickness. This is particularly noticeable when more than one single layer is used. In principle this is similar to the limitation existing on the determination of layers thicknesses from the reflectivity interference fringes when multiple layers exist. However FD-FFOCT has the advantage of minimizing the effect of multiple interferences when the coherence length is much smaller than the layers thickness.

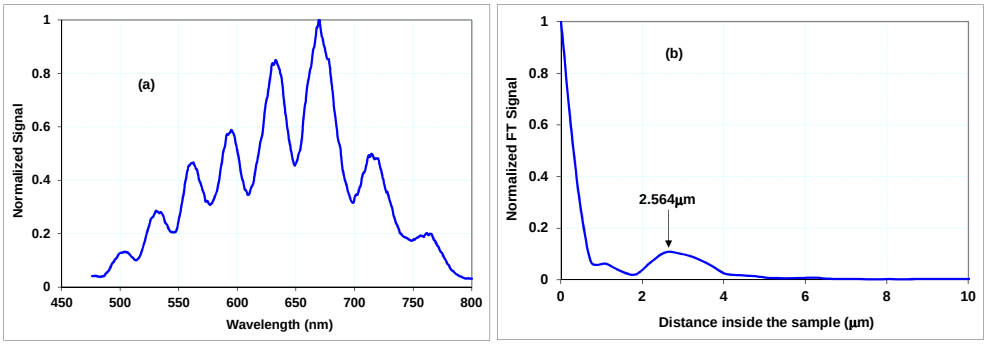

Figure 5. (a) FDOCT signal obtained from SiO2 layer on Si using Mirau microscope and (b) Its Fourier transform.

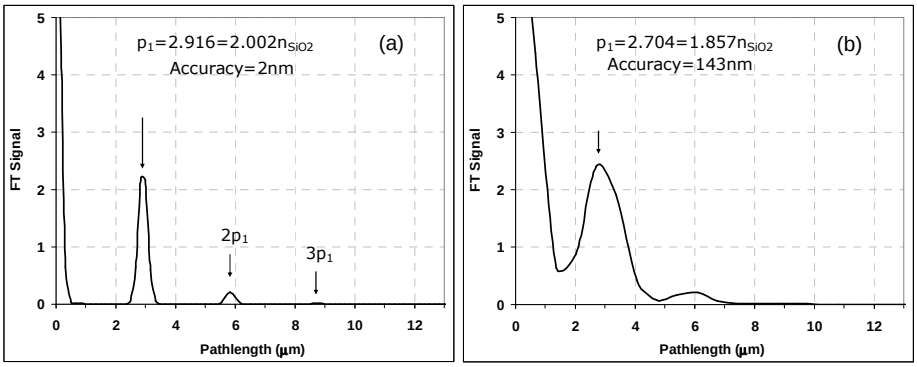

Figure 6. (a) FD-OCT signal from a 2µm SiO2 layer on Si using Gaussian source centered at 600nm having bandwidth of 400nm showing the effect of multiple interferences. The indices used are 1.456 for the oxide and 3.94 for the Si. (b) Same as in (a) but with bandwidth of 110nm.

Another potential approach is to solve the inverse scattering problem for the interference signal in a similar manner to spectroscopic ellipsometry and polarized reflectometry. This approach was proposed[42] a decade ago using an interference microscope with annular lenses and applied to SiO_2 on Si substrate. It consists of measuring the spectroscopic interferogram (spectrogram), building a model to the structure including refractive index dispersions and perform fitting between the model and the measurement to find the parameters of the layered structure. Although refractive index dispersions have been measured with WLI[43], the use of annular lenses is again suggested to simplify the simulations and allow 3D thickness mapping. Another advantage of using the inverse scattering approach together with annular lenses is the fact that the depth of focus is extended by the factor of $1/\sqrt{1-\varepsilon^2}$ which is more than factor of

two for $\varepsilon = 0.9$. This fact is important particularly with FD-FFOCT as one need to have all the sample layers in focus. For the 2μm single layer of oxide mentioned above the two interfaces will then be in focus simultaneously and one can model its reflectivity easily using Airy formulae for thin films with incidence angle equals nearly to $\theta_{inc} \approx (\theta_{\varepsilon} + \theta_{max})/2$. According to equation (1) if we choose $\delta z = 0$, the spectrogram will then be similar to that from a Michelson interferometer. In figure 7a the spectrogram from the oxide layer with different thicknesses 2000nm, 2050nm and 2100nm is calculated for $\theta_{inc} = 59.12^{\circ}$ corresponding to NA=0.9 and $\varepsilon = 0.9$. The reflectivity for p-polarized light was calculated and the normalized spectrogram was found from $\left|r_r + r_p\right|^2 / 4$ where $r_r = 0.5$ chosen so that the contrast of the fringes of the spectrogram is maximized. In comparing with the reflectivity itself shown in figure 7b, it is evident that the spectral interference approach enhances the fringes contrast and the sensitivity to thickness variations. Hence the use of inverse scattering together with spectral interference microscopy using annular lenses could be a powerful technique for thin films thickness mapping with high accuracy and high resolution.

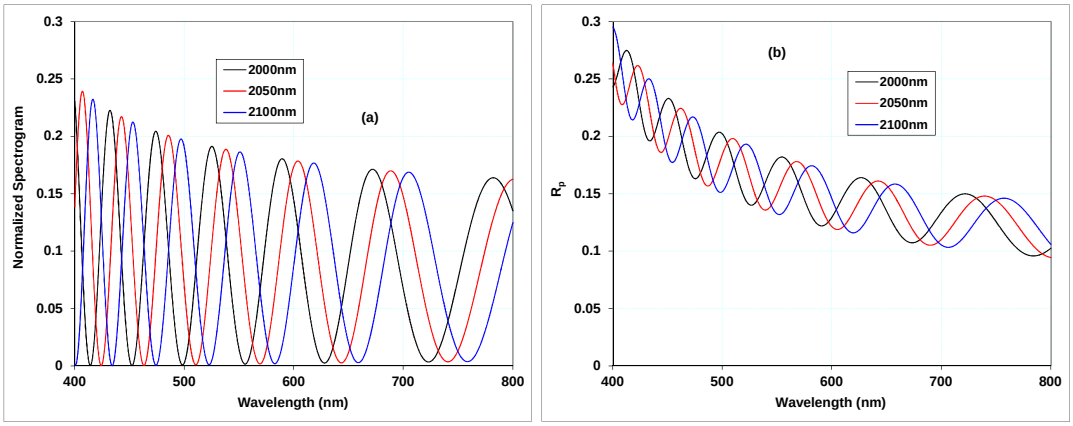

Figure 7. Demonstration of the inverse scattering approach using annular lens with NA=0.9 and $\varepsilon = 0.9$ where incidence angle taken corresponds to the center of the annulus. The structure is a 2μm SiO2 layer on Si substrate and using gaussian source centered at 600nm with 200nm bandwidth. (a) Spectrograms for p-polarized light from three thicknesses different from the nominal by 50nm, showing the high sensitivity to thickness variations while (b) shows the p-polarized reflectivity. Comparison between (a) and (b) demonstrates clearly the power of the spectrogram approach over polarized reflectivity approach. The reference mirror reflectivity was chosen 0.25 to maximize the contrast in the spectrogram fringes.

III. RECENT DEVELOPMENTS AND DISCUSSION OF LIMITATIONS

During the last decade significant improvements to the LCM methodologies emerged as a result of the continuous interest in FFOCT as highly promising technique to obtain high resolution 3D images in real time. Path length modulation techniques and algorithms were developed to improve the signal to noise ratio as well as dynamic focusing allowed increasing the imaging depth inside tissue[35-38, 44,45,46]. . When the numerical aperture (NA) of the microscope objectives used becomes large (0.7 or larger) several limitations arise which need to be considered carefully. Competition between the longitudinal spatial coherence and the temporal coherence takes place and affect thickness measurement using FFOCT. In our recent studies we have addressed part of these limitations in order to improve the performance of full field LCMs. The following is a list of consequences and statements that help in understanding these limitations and for details the readers are referred to reference[11]:

1. Fringe size: A parameter of particular interest when working with monochromatic light is the fringe size, which is the distance between two maxima or two interference minima. Without the effect of the spatial coherence this is supposed to be $\lambda/2$, however due to spatial coherence it is decreased to $\lambda/2\eta$ where $\eta \geq 1$ is called the fringe size correction factor. A more accurate formulae for the fringe size was derived by us recently taking into account the spatial coherence effects[10,47]:

$$\eta = \frac{2}{1+\cos\alpha_0 + \sigma^2 \sin^2(\alpha_0/2)} \tag{2}$$

Where here $\sin\alpha_0 = NA$ and σ is the coherence factor which was found to be around 0.5-0.75 for best fit to the existing experimental data.

2. Longitudinal spatial coherence takes an effect when the path length scan is performed with non-collimated beam such as defocus scan of a lens where the focal depth of the lens mainly determines the coherence region. The longitudinal coherence length is determined basically by the focal depth of the microscope objective (NA, λ, and the refractive index of the object space).

3. For each temporal coherence length there is a minimum NA value above which the interferogram starts to narrow due to the spatial coherence. In other words for each NA value there is a limit on the temporal coherence length above which its effect on the interferogram width starts to diminish. In this case the fringe size for a monochromatic light is smaller than half the wavelength by a factor determined by the spatial coherence.

4. The lateral alignment between the main and reference wavefronts is crucial for the best performance of FF-OCT system as the lateral coherence region on the sample is comparable to the radius of the Airy function.

5. When imaging a multilayered sample with FF-OCT the relation between the maximum contrast position and layer thickness is different from the case of collimated beam OCT that relies on the low temporal coherence (equations (3) and (4)). In the case of low NA so that the temporal coherence length is much shorter that the spatial coherence length layers thicknesses are determined from the relation:

$$d_j = (n_0 / n_j)\delta z_j \tag{3}$$

Where here n_0, n_j are the refractive indices of the medium above the sample and of layer j in a multilayered sample. δz_j is the axial scan required in order to obtain best interferogram contrast. On the other hand when the spatial coherence is the dominant this relation becomes:

$$d_j = (n_j / n_0)\delta z_j \tag{4}$$

This difference was confirmed experimentally recently by Safrani and Abdulhalim[44,45] and relation (3) was generalized to the case of multilayers.

6. When multilayered samples are imaged the imaging depth is limited due to several factors: (6.1) Mismatch of the main and reference pathlengths as the focused beam penetrates deeper into the layers, (6.2) Dispersion effects of the sample, which become more severe when the bandwidth is wide and the NA is high. Although results on the dispersion effects are not shown here, they were discussed heavily by us[10] including the chromatic aberrations effects, (6.3) Multiple interference effects when the sample is non-scattering and (6.4) Mismatch between the spatial coherence and the temporal coherence interferograms which becomes more severe when the longitudinal spatial and temporal coherence lengths are short and comparable.

To conclude, interference microscopy based on low coherence has undergone major improvements during the last decade due to the emergence of OCT as a powerful technique for 3D imaging of scattering layered media. The optical metrology applications of LCMs such as the Linnik, the Mirau or the Taylor microscopes will as a result be enhanced. When combined with fast tunable lasers, tunable filters or imaging spectrometers these tools will give high resolution images in real time and in many aspects might replace confocal microscopy. Lowering the wavelength and increasing the NA will improve the lateral and axial resolutions significantly as it was demonstrated recently[48] using the Linnik microscope with UV LED. Techniques for superresolution and extending the depth of focus[49,50,51] can also enhance the functionality of LCMs.

Acknowledgement. This work was supported partially by the Ministry of Science, Israel under the *Tashtiot program*. I am grateful to my students, who enhanced this research activity during the last few years: Ron Friedman, Ronen Dadon, Lior Liraz, Jenny Sokolovsky and Avner Safrani.

REFERENCES

[1] Gasvik, K.J., [Optical Metrology], 3rd ed., Wiley, New York, (1996).
[2] Tompkins, H. G., [A User's Guide to Ellipsometry], Academic, New York, (1993).
[3] Pluta, M, [Advanced Light Microscopy], Polish Scientific Publishers,Warsaw, Vol. 3, pp. 265–271 (1993).
[4] Gu, M., [Principles of Three Dimensional Imaging in Confocal Microscopes], World Scientific, Singapore, (1996).
[5] Wilson, T., and Shippard, C. J. R., [Theory and Practice of Scanning Optical Microscopy], Academic, London (1984).
[6] Krug, W., Rienitz, J., and Schultz, G. (eds), [Contributions to Interference Microscopy], Hilger and Watts, London (1964).
[7] Sheppard, C. J. R. and Zhou, H., "Confocal interference microscopy," Proc. SPIE 2984, 85–89 (1997).
[8] Davidson, M., Kaufman, K., Mazor, I., and Cohen, F. "An application of interference microscopy to integrated circuit inspection and metrology," Proc.SPIE 775, 233–247 (1987).
[9] Abdulhalim, I., "Coherence effects in applications of frequency and time domain full field optical coherence tomography to optical metrology," J. Holography and Speckle, 5, 180-190 (2009).
[10] Abdulhalim, I., "Theory for Double Beam Interferometric Microscopes and Experimental Verification using the Linnik Microscope," J.Mod.Optics 48 (2) 279-302 (2001).
[11] Abdulhalim, I., "Spatial and temporal coherence effects in interference microscopy and full-field optical coherence tomography," Ann. Der Physik, 524, 787-804 (2012).
[12] 'Technology Roadmap for Nanoelectronics', European Commission, November 2000. Webpage http://cordis.europa.eu/ist/.
[13] Raymond, C. J., Murnane, M. R., Naqvi, S. S. H., and McNeil, J. R., "Metrology of subwavelength photoresist gratings using optical scatterometry," J. Vacuum Sci. Technol. B 13, 1484–1495 (1995).
[14] Abdulhalim, I., "Simplified optical scatterometry for periodic nano-arrays in the quasi-static limit," Appl.Opt., 46, 2219-2229 (2007).
[15] Abdulhalim, I., Adel, M., Friedmann, M., and Faeyrman, M., "Periodic Patterns and Techniques to Control Misalignment," US Patents Application #2003/0002043 A1, Jan. 2, (2003).
[16] Huang, H-T., Kong, W., and Terry Jr. F. L., "Normal Incidence Spectroscopic Ellipsometry for Critical Dimension Monitoring," Applied Physics Letters, 78, 3983-3985 (2001).
[17] Xu, Y., and Abdulhalim, I., "Spectroscopic Scatterometer System,", U.S. Patents No' 6,483,580 Nov. 19, (2002).
[18] Abdulhalim, I., Auslender, m., and Hava, S., "Resonant and scatterometric gratings based nano-photonic structures for biosensing," Journal of NanoPhotonics, 1, 011680 (2007).
[19] Danielson, B. L., and Boisrobert, C. Y., "Absolute optical ranging using low coherence interferometry," Appl. Opt. 30, 2975–2979 (1991).
[20] Dresel, T., Hausler, G., and Venzke, G., "Three-dimensional sensing of rough surfaces by coherence radar," Appl. Opt. 31, 919–925 (1992).
[21] Deck, L., and de Groot, P., "High-speed noncontact profiler based on scanning white-light interferometry," Appl. Opt. 33, 7334–7338 (1994).
[22] de Groot, P., and Deck, L., "Three-dimensional imaging by sub-Nyquist sampling of white-light interferograms," Opt. Lett. 18, 1462–1464 (1993).
[23] Chen, S., Palmer, A. W., Grattan, K. T. V., and Meggitt, B. T., "Digital signal-processing techniques for electronically scanned optical-fiber white-light interferometry," Appl. Opt. 31, 6003–6010 (1992).
[24] Gale, D., Pether, M. I., and Dainty, J. C., "Linnik microscope imaging of integrated circuit structures," Appl. Opt. 35, 131-148 (1996).
[25] Chim, S. S. C., and Kino, G. S., "Mirau correlation microscope," Opt. Lett. 15, 579–581 (1990).
[26] Huang, D., Swanson, E. A., Lin, C. P., Schuman, J. S., Stinson, W. G., Chang, W., Lee, M. R., Flotte, T., Gregory, K., Puliafito, C. A., and Fujimoto, J. G., "Optical coherence tomography," Science 254, 1178–1181 (1991).

[27] Swanson, E. A., Izatt, J. A., Hee, M. R., Huang, D., Lin, C. P. Schuman, J. S., Puliafito, C. A., and Fujimoto, J. G., "*In vivo* retinal imaging by optical coherence tomography," Opt. Lett. 18, 1864-1866 (1993).
[28] Bouma, B. E., and Tearney, G. J., eds., [Handbook of Optical Coherence Tomography], Marcel Dekker, New York, (2002).
[29] Fercher, A.F., Drexler, W., Hitzenberger, C. K., and Lasser, T., "Optical coherence tomography-principles and applications," Rep. Prog. Phys. 66, 239–303 (2003).
[30] Zysk, A.M., Nguyen, F.T., Oldenburg, A. L., Marks, D.L., Boppart, S.A., "Optical coherence tomography: a review of clinical development from bench to bedside," Journal of Biomedical Optics 12 (5) 051403-21 (2007).
[31] Hausler, F., and Lindmer, M. W., "Coherence radar and spectral radar—new tools for dermatological diagnosis," J. Biomed. Opt. 3, 21–31 (1998).
[32] Dorrer, C., Belabas, C., Likforman, J.-P. and Joffre, M., "Spectral resolution and sampling issues in Fourier-transform spectral interferometry," J. Opt. Soc. Am. B 17, 1795–1802 (2000).
[33] Wojtkowski, M., Srinivasan, V. J., Ko, T. H., Fujimoto, J. G., Kowalczyk, A., and Duker, J. S. "Ultrahigh-resolution, high speed, Fourier domain optical coherence tomography and methods for dispersion compensation," Opt. Express 12, 2404 – 2422 (2004).
[34] Hu, Z., and Rollins, A. M., "Theory of two beam interference with arbitrary spectra," Opt. Express 14, 12751–12759 (2006).
[35] Dubois, A., Grieve, K., Moneron, G., Lecaque, R., Vabre, L., and Boccara, A. C. "Ultrahigh-resolution full-field optical coherence tomography," Appl. Opt. 43, 2874-2883 (2004).
[36] Oh, W. Y., Bouma, B. E., Iftimia, N., Yun, S. H., Yelin, R., and Tearney, G. J., "Ultrahigh-resolution full-field optical coherence microscopy using InGaAs camera," Optics Express 14, 726-735 (2006).
[37] Laude, B., De Martino, A., Drevillon, B., Benattar, L., and Schwartz, L., "Full-field optical coherence tomography with thermal light," Appl. Opt. 41, 6637-6645 (2002).
[38] Moneron, G., Boccara, A. C., and Dubois, A., "Stroboscopic ultrahigh-resolution full-field optical coherence tomography," Opt. Lett. 30, 1351-1353 (2005).
[39] Pfortner, A., and Schwider, J., "Dispersion error in white-light Linnik interferometers and its implications for evaluation procedures," Appl.Opt. 40 (34) 6223-6228 (2001).
[40] Abdulhalim, I., "Method for the measurement of multilayers refractive indices and thicknesses using interference microscopes with annular aperture," Optik, 110 (10), 476-8 (1999).
[41] Kim, S-W., and Kim, G-H. "Thickness-profile measurement of transparent thin-film layers by white-light scanning interferometry," Appl.Opt. 38, (28) 5968-5973 (1999).
[42] Abdulhalim, I., "Spectroscopic Interference Microscopy Technique for Measurement of layer Parameters," Meas.Sci.Technol., 12, 1996-2001 (2001).
[43] Diddams, S., and Diels, J. C., "Dispersion measurements with white-light interferometry," J. Opt. Soc. Am. 13, 1120–1129 (1996).
[44] Safrani, A. and Abdulhalim, I., "Spatial coherence effect on layers thickness determination in narrowband full field optical coherence tomography," Applied Optics 50, 3021-27 (2011).
[45]Safrani, A., and Abdulhalim, I., "Ultra High Resolution Full Field Optical Coherence Tomography Using Spatial Coherence Gating and Quasi Monochromatic Illumination," Opt. Lett. 37, 458 (2012).
[46] Sokolovsky, J., Yitzhaky, Y., and Abdulhalim, I., "Analysis of Optical Coherence Tomography Interferograms of Multi-Layered Biological Samples," Appl.Opt., 51, 8390-8400 (2012).
[47] Abdulhalim, I., "Competence between spatial and temporal coherence in full field optical coherence tomography and interference microscopy," J. Opt. A: Pure Appl. Opt. 8, 952-958 (2006).
[48] Niehues, J., Lehmann, P., and Xie, W., "Low coherent Linnik interferometer optimized for use in nano-measuring machines," Meas. Sci. Technol. 23, 125002 (9pp) (2012).
[49] Zlotnik, A., Abraham, Y., Liraz, L., Abdulhalim, I., and Zalevsky, Z., "Improved Extended Depth of Focus Full Field Spectral Domain Optical Coherence Tomography," Opt.Commu. 283, 4963-68 (2010).
[50] Sharon, R., Friedmann, R., Abdulhalim, I., "Multilayered scattering reference mirror for full field optical coherence tomography with application to cell profiling," Opt.Commu. 283, 4122-25 (2010).
[51] Abdulhalim, I., Friedman, R., Liraz, L., and Dadon, R., "Full field frequency domain common path optical coherence tomography with annular aperture," Proc. SPIE, 6627, 662719 (2007).